Detection and Identification of Rare Audiovisual Cues

Insperata accident magis saepe quam quae speres.
(Things you do not expect happen more often than
things you do expect) Plautus (ca 200(B.C.))

Project no: 027787

DIRAC

Detection and Identification of Rare Audio-visual Cues

Integrated Project
IST - Priority 2

DELIVERABLE NO: D4.16

CURRENT SOURCE DENSITY ANALYSIS OF AUDITORY CORTEX

Date of deliverable: 30.6.2010
Actual submission date: 12.8.2010

Start date of project: 01.01.2006 Duration: 60 months

Organization name of lead contractor for this deliverable: **LIN**

Revision [0]

Project co-funded by the European Commission within the Sixth Framework Program (2002-2006)		
Dissemination Level		
PU	Public	
PP	Restricted to other program participants (including the Commission Services)	
RE	Restricted to a group specified by the consortium (including the Commission Services)	X
CO	Confidential, only for members of the consortium (including the Commission Services)	

D4.16 CURRENT SOURCE DENSITY ANALYSIS OF AUDITORY CORTEX

Leibniz Institute for Neurobiology (LIN)

Abstract:

Primary sensory cortex integrates sensory information from afferent feedforward thalamocortical projection systems and convergent intracortical microcircuits. Both input systems have been demonstrated to provide different aspects of sensory information. We therefore aimed at revealing the functional microcircuitry in primary auditory cortex underlying the integration of spectral information as a model mechanism of how topographically organized representations of stimulus features, derived from the biophysical constraints of sensory transduction processes and subsequent neuronal computations, emerge on early cortical sensory processing level. In a recent study, we have used high-density recordings of laminar current source density (CSD) distributions in primary auditory cortex of Mongolian gerbils in combination with pharmacological silencing of cortical activity and analysis of the residual CSD, to dissociate the feedforward thalamocortical contribution and the intracortical contribution to spectral integration (Happel et al., 2010). We found a temporally highly precise integration of both types of inputs when the stimulation frequency was in close spectral neighborhood of the best frequency of the measurement site, where the overlap between both inputs is maximal. Local intracortical connections provide both, directly feedforward excitatory and modulatory input from adjacent cortical sites, which determine how concurrent afferent inputs are integrated. Through separate excitatory horizontal projections, terminating in cortical layers II/III, information about stimulus energy in greater spectral distance is provided even over long cortical distances. The analysis of the spatial and temporal interaction of the aforementioned subsystems allowed us to propose a conceptual framework of spectral integration in AI that includes different and partly controversial anatomical and physiological models in the literature.

In this deliverable, we present a short summary of the main results. For a more detailed overview of the study please see Happel et al., (2010).

Table of Content

1. Introduction

Primary sensory cortices have been described to display topographically organized representations of specific stimulus features, as the spectral distribution of acoustic signal energy in the case of auditory cortex, dominantly represented in tonotopic maps (for overview see Schreiner and Winer, 2007). Within this tonotopic map information from different parts of the signal spectrum is integrated by different input subsystems, called spectral integration. Previous studies investigated this on the level of single unit firing behavior (e.g. Ohl & Scheich, 1997; Schreiner et al., 2000; Miller et al., 2001a,b; Kadia and Wang, 2003) and on the subthreshold integration of inputs with cell-attached recording (Wehr and Zador, 2003; Liu et al., 2007) or recording of local field potentials (LFPs) (Kaur et al., 2004, 2005; Metherate et al., 2005). They revealed that the fine-grained suprathreshold representation of frequencies in primary auditory cortex cannot exclusively be inherited from afferent feedforward inputs (Miller et al., 2001; Edeline, 2003; Wehr and Zador, 2003; Winer et al., 2005, Bitterman et al., 2008), but that different short-range or long-range intracortical connections could potentially also provide spectral input to a given cortical site (Wallace et al., 1991; Budinger et al, 2000). Intracortical inputs could provide (subthreshold) spectral input to adjacent cortical regions not receiving any corresponding thalamic input (Metherate et al., 2005; Kurt et al., 2008; Moeller et al., 2010) or sharpen cortical frequency tuning by intracolumnar circuits which mediate excitation through recurrent loops that selectively amplify suprathreshold activation of thalamocortical input (Liu et al., 2007).

These data raise the question how the integration of information about the stimulus spectrum from thalamocortical inputs and intracortical inputs is organized in time and space, i.e. across the synaptic populations extending over the dendritic tree of cortical principal neurons. To answer this question, we have shown in a recent report (Happel et al., 2010), using analysis of the pure-tone-evoked laminar profiles of tone-evoked current source density (CSD) in combination with pharmacological cortical silencing, that afferent thalamocortical inputs and convergent intracortical inputs have a discernible spatial organization and are differentially recruited in time. Specifically, when a cortical site was stimulated with a tone frequency corresponding to its best frequency (BF) or to a spectrally distant frequency (nonBF), we found thalamocortical or intracortical inputs, respectively, to be the dominant generators of the initial cortical activation. For frequencies in the spectral neighborhood of the BF (nearBF), where both input systems exhibit their greatest overlap, we found a temporally highly precise integration of both inputs to produce a characteristic laminar activation profile.

2. Methods

2.1 Current source density analysis

Based on laminar local field potential (LFP) recordings we calculated the one-dimensional current-source density (CSD) profile from the second spatial derivative of the LFP (Mitzdorf, 1985, 1986; Steinschneider et al., 1992):

$$-CSD \approx \frac{\delta^2 \phi(z)}{\delta z^2} = \frac{\phi(z+n\Delta z) - 2\phi(z) + \phi(z-n\Delta z)}{(n\Delta z)^2} \quad (1)$$

where Φ is the field potential, z the spatial coordinate perpendicular to the cortical laminae, Δz the sampling interval (55-75 μm), and n the differentiation grid.

2.1.1 Averaged rectified CSD and residue analysis

The averaged rectified CSD (AVREC, Givre et al., 1994, Schroeder et al., 1998) was calculated by averaging the absolute values of the CSD separately across the n channels for each trial. Subsequently, data were averaged across trials (2). While information about the direction of transmembrane current flow is lost by rectification, the resulting AVREC waveform provides a measure of the temporal pattern of the overall strength of transmembrane current flow (Givre et al., 1994, Schroeder et al., 1998). The relative CSD residues (Harding, 1992) were calculated as the sum of the CSDs over the n channels divided by the sum of the respective absolute values (3).

$$AVREC = \frac{\sum_{i=1}^{n} |CSD_i|(t)}{n} \quad (2)$$

$$relative\ \ residues = \frac{\sum_{i=1}^{n} CSD_i(t)}{\sum_{i=1}^{n} |CSD_i|(t)} \quad (3)$$

2.2 Pharmacological silencing

Intracortical neuronal activity was inhibited using 20 µl of the $GABA_A$-agonist muscimol hydrobromide with a concentration of 0.2-1.0 µg/µl applied topically onto the dura. In some cases (n=3) we concomitantly applied with $GABA_B$-receptor agonist (+)-5,5-dimethyl-2-morpholine acetic acid (SCH50911; 6 mM, 20 µl), since muscimol alone potentially activates $GABA_B$-receptors (EC_{50}=25 µM, Yamauchi et al., 2000), which would create thalamocortical EPSPs smaller in amplitude due to presynaptic inhibition (Liu et al, 2007). In all cases we found a strong effect of response inhibition of the laminar LFP and CSD profiles.

3. Conclusion

3.1 Cortical silencing to dissociate thalamocortically and intracortically evoked CSD components

We have investigated the laminar organization of afferent thalamocortical input and convergent inputs from the intracortical microcircuitry in gerbil primary auditory cortex. Laminar current source density (CSD) profiles in AI have been evoked by pure tones using a wide range of frequencies. To dissociate thalamocortical input to primary sensory cortex from horizontal intracortical synaptic interactions we applied the $GABA_A$-receptor agonist muscimol alone (0.2-1 µg/µl, see Talwar et al., 2001; Kaur et al., 2004) or concomitantly with the $GABA_B$-antagonist SCH50911 (1:1.5, Yamauchi et al., 2000) topically onto the cortical surface.

The CSD profile after BF stimulation in the untreated auditory cortex (Fig. 1A) indicates feedforward input from afferent thalamocortical projections terminating in granular layers III/IV and also intracortical connections to supragranular and infragranular layers (see Fig. 1A, left).

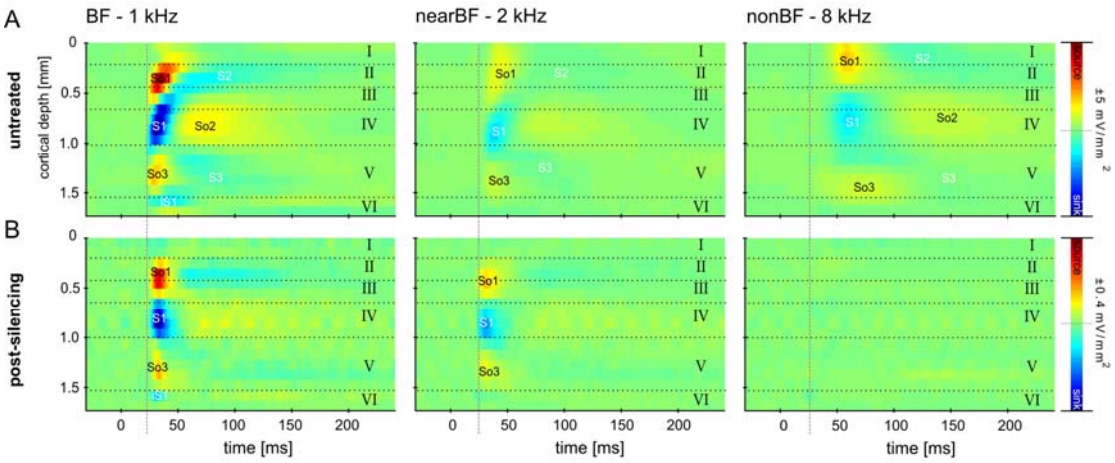

Figure 1: Dissociation of thalamocortical and intracortical contributions of the laminar CSD profile. ***A***, Laminar processing in AI differed with stimulation frequency (BF, near-best frequency, nearBF, or non-best frequency, nonBF, stimulation). ***B***, after cortical silencing remaining sinks were observed exclusively after BF and nearBF stimulation in thalamocortical input layer IV (>30 minutes, see Fig. 1). Activations after nonBF stimulation were abolished completely. Note that the onset latency of the nearBF-evoked initial granular sink S1 was faster after drug application. In contrast cortical silencing had no effect on the onset latency of BF-evoked S1 (see dashed line as reference).

We found pure tone frequencies of 1 octave distance to evoke significantly different CSD profiles (nearBF-stimulation), indicative of activation of different synaptic populations, in accordance with our previous results on the tonotopic organization of tone-evoked local field potentials in gerbil primary auditory cortex field AI (Ohl et al. 2000a,b). Furthermore, the initial response was found in granular layers irrespective of stimulation frequency, indicating that initial activation in granular layers need not be a unique feature of profiles evoked by afferent thalamocortical input, but could also occur in profiles with a considerable amount of initial horizontal intracortical input.

Using the described cortical silencing method we aimed at dissociating the contribution of subcortical feedforward input to cortical CSD profiles evoked with different stimulation frequencies from contributions of convergent intracortical input. The robust granular sink S1 indicates activation of synapses mainly within layer IV which is believed to be the major laminar recipient of tonotopically

organized afferent input from the ventral part of the medial geniculate body (vMGB; Budinger et al., 2000; Hackett, 2010). We found this thalamocortical input after BF- and nearBF-stimulation. Activations after nonBF-stimulation were silenced completely (Fig. 1B).

3.2 Temporal precision of afferent and local horizontal convergent input

While existing data already indicate a division of labor between thalamocortical and intracortical input systems for processing BF and nonBF stimuli, respectively, it is not fully understood how spectral integration is achieved in the nearBF region where thalamocortical and intracortical input systems have their greatest overlap (see Fig. 1, middle panel).

Further insight into the functional convergence of thalamocortical and horizontal intracortical contributions was obtained from the analysis of the averaged rectified CSD (AVREC), as a measure of the temporal current flow of overall evoked activity (Givre et al., 1994; Schroeder et al., 1998) and of the relative residues of the CSD (Harding 1992).

Since activation of presynaptic terminals with its accompanying massive calcium influx contributes significantly to the LFP (Tenke et al. 1993; Stoelzel et al. 2008), the largely orthogonal orientations of thalamocortical and intracortical input systems can be expected to contribute differently to the relative residues of the CSD as measured with a linear electrode array oriented perpendicular to the cortical surface (see Fig. 2A). Specifically, it can be hypothesized that activation of the horizontal intracortical input contributes more to the relative residues than activation of the thalamocortical input (see schematic traces in Fig. 2A), because, current sources and sinks that cancel each other out are more likely to be distributed beyond the cylinder surrounding the electrode array where extracellular currents would most contribute to the measured local field potential.

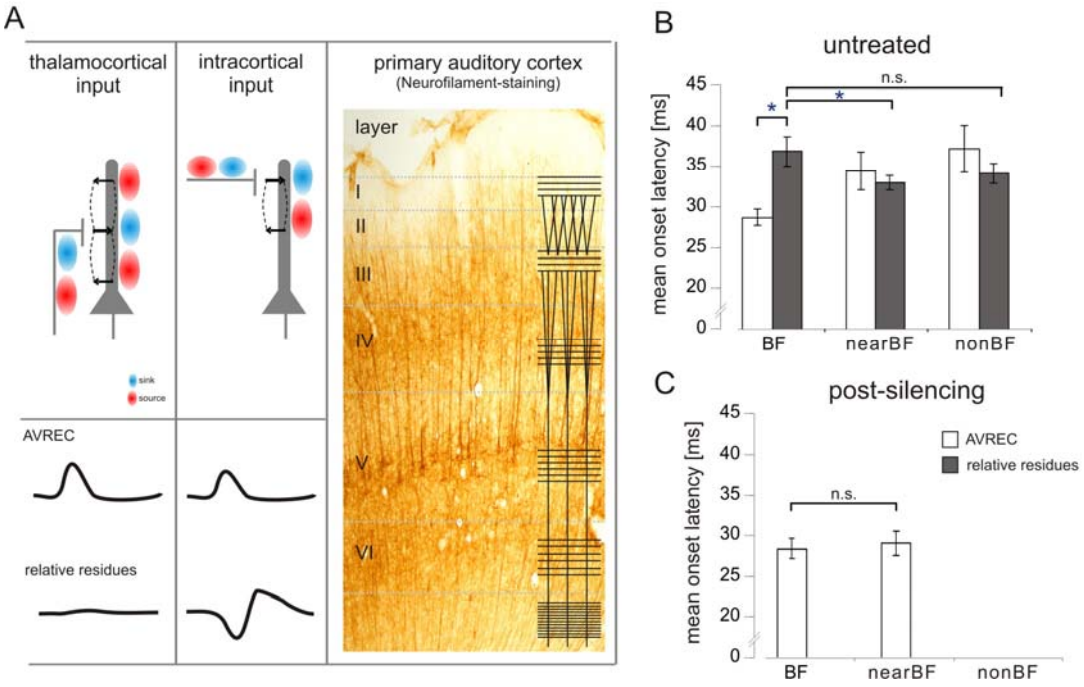

Figure 2: Using the residual CSD for dissociating thalamocortical and intracortical contributions to the laminar activation profile. ***A***, *Left*, The averaged rectified CSD (AVREC) waveform reflects the temporal characteristics of the overall current flow at a given measurement site (Givre et al., 1994, Schroeder et al., 1998). Relative residues of the CSD, reflect the amount of unbalanced sinks and sources (Harding, 1992). The mutually largely orthogonal orientations of thalamocortical and intracortical input systems can be expected to contribute differently to the relative residues of the CSD measured with a linear electrode array oriented perpendicular to the cortical surface (see traces). *Right*, Visualization of the orthogonal thalamocortical and intracortical fiber orientation using SMI32 neurofilament staining of gerbil primary auditory cortex (courtesy of Dr. Eike Budinger) reflecting the canonical pattern of fiber orientations in sensory neocortex (overlaid line schematic after Creutzfeldt, 1983). For further explanation see text. ***B***, Mean onset latencies (±SEM) of AVREC were significantly shorter for BF stimulation (paired t-test, p=0.0006), but AVREC and relative residues showed no significant differences for near/nonBF stimulation. Mean onset latencies (±SEM) of relative residues showed significant differences for BF vs. nearBF stimulation (p=0.023), but were not significantly different for BF vs. nonBF stimulation (p=0.173). ***C***, Cortical silencing blocked all tone-evoked relative residues. Significant AVREC values vanished also for nonBF stimulation. AVREC mean onset latencies for BF and nearBF stimulation showed no significant difference (p=0.43), (* paired t-test, $p<0.05$).

We found markedly different latency profiles of AVREC and relative residues dependent on stimulus condition. AVREC leads the relative residues in time for BF stimulation, while AVREC and the relative residues show equal onset latencies for near/nonBF stimulation. After cortical silencing, AVREC was greatly reduced, but significant amplitudes were found for a narrow band of stimulation frequencies in the BF region (for quantification see Happel et al., 2010). In agreement with the hypothesis, relative residues were completely abolished by silencing of intracortical inputs.

Eventually, we showed that potentially anatomically overlapping afferent thalamocortical and intracortical pathways are recruited in a way such that both input systems interact and shape the initial response in primary auditory cortex in dependence on the stimulation frequency. Specifically, horizontal inputs terminating in the (upper) granular layers interact directly with afferent inputs when the stimulation frequency is not the BF. In the latter case, afferent input activates a cortical site without convergent horizontal interactions.

From the present data on spatial (laminar) and temporal organization of spectral integration, we propose that information about the spectral energy distribution of sounds is integrated by at least four different input systems: (1) afferent thalamocortical input to granular layers (Budinger et al, 2000; Hacket, 2010), (2) intracolumnar excitation through local intracortical recurrent microcircuits (Liu et al., 2007), (3) convergent local horizontal intracortical connections between neighboring columns (Ojima et al., 1991; Budinger et al., 2000). (4) Additionally, long-range horizontal connections potentially contribute to the edges of the subthreshold RF via excitatory connections (Metherate et al., 2005; Kurt et al., 2008; Moeller et al., 2010). Initial nearBF-evoked responses thus appear to result from a precise, spatiotemporally organized recruitment of both afferent thalamocortical and intercolumnar local horizontal inputs.

For a more elaborate presentation see Happel et al., 2010.

4. References

Bitterman Y, Mukamel R, Malach R, Fried I, Nelken I (2008) Ultra-fine frequency tuning revealed in single neurons of human auditory cortex. Nature 451(7175):197-201.

Budinger E, Heil P, Scheich H (2000) Functional organization of auditory cortex in the Mongolian gerbil (Meriones unguiculatus). III. Anatomical subdivisions and corticocortical connections. Eur J Neurosci 12(7):2425-2451.

Edeline JM (2003) The thalamo-cortical auditory receptive fields: regulation by the states of vigilance, learning and the neuromodulatory systems. Exp Brain Res 153(4):554-572.

Givre SJ, Schroeder CE, Arezzo J (1994) Contribution of extrastriate area V4 to the surface-recorded flash VEP in the awake macaque. Vis Res 34:415-438.

Hackett TA (2010) Information flow in the auditory cortical network. Hear Res doi:10.1016/j.hearres.2010.01.011

Happel, MFK., Jeschke, M., Ohl, FW. (2010) Spectral integration in primary auditory cortex Attributalbe to temporally precise convergence of thalamocortical and intracortical input. J Neurosci. In press

Harding, GW (1992) The currents that flow in the somatosensory cortex during the direct cortical response. Exp Brain Res 90(1):29-39.

Kaur S, Lazar R, Metherate R (2004) Intracortical pathways determine breadth of subthreshold frequency receptive fields in primary auditory cortex. J Neurophysiol 91(6):2551-2567.

Kurt S, Deutscher A, Crook JM, Ohl FW, Budinger E, Moeller CK, Scheich H, Schulze H (2008) Auditory Cortical Contrast Enhancing by Global Winner-Take-All Inhibitory Interactions. PLoS ONE 3(3): e1735.

Liu B, Guangying KW, Arbuckle R, Huizhong WT, Zhang LI (2007) Defining cortical frequency tuning with recurrent excitatory circuitry. Nat Neurosci 10(12):1594-600.

Metherate R, Kaur S, Kawai H, Lazar R, Liang K, Rose H (2005) Spectral integration in auditory cortex: Mechanisms and modulation. Hear Res 206(1-2):146-158.

Miller L, Escabi M, Read H, Schreiner C (2001) Functional convergence of response properties in the auditory thalamocortical system. Neuron 32(1):151160.

Mitzdorf U (1986) The physiological causes of VEP: current source density analysis of electrically and visually evoked potentials. In: Evoked Potentials (Cracco R, Bodis-Wollner I, ed), pp 141-154, New York, Allan R. Liss.

Mitzdorf U (1985) Current source-density method and application in cat cerebral cortex: investigation of evoked potentials and EEG phenomena. Physiol Rev 65(1):37-100.

Moeller CM, Kurt S, Happel MFK, Schulze HS (2010) Long-range effects of GABAergic inhibition in gerbil primary auditory cortex. Eur J Neurosci 31(1):49-59.

Ojima H, Honda CN, Jones EG (1991) Patterns of axonal collateralization of identified supragranular pyramidal neurons in the cat auditory cortex. Cereb Cortex 1:80-94.

Ohl FW, Scheich H, Freeman WJ (2000a) Topographic analysis of epidural pure-tone-evoked potentials in gerbil auditory cortex. J Neurophysiol 83(5):3123-3132.

Ohl FW, Schulze H, Scheich H, Freeman WJ (2000b) Spatial representation of frequency-modulated tones in gerbil auditory cortex revealed by epidural electrocorticography. J Physiol Paris 94(5-6):549-554

Schroeder CE, Mehta AD, Givre SJ (1998) A spatiotemporal profile of visual system activation revealed by current source density analysis in the awake macaque. Cereb Cortex 8(7):575-92.

Stoelzel CR, Bereshpolova Y, Gusev AG, Swadlow HA (2008) The impact of an lgnd impulse on the awake visual cortex: synaptic dynamics and the sustained/transient distinction. J Neurosci 28(19):5018-5028.

Tenke CE, Schroeder CE, Arezzo JC, Vaughn HG (1993) Interpretation of high-resolution current source density profiles: a simulation of sublaminar contributions to the visual evoked potential. Exp Brain Res 94:183-192.

Wehr, M. & Zador, A. (2003) Balanced inhibition underlies tuning and sharpens spike timing in auditory cortex. Nature, 426: 442-446.

Winer JA, Miller LM, Lee CC, Schreiner CE (2005) Auditory thalamocortical transformation: structure and function. TINS 28(5):255-263.

Yamauchi T, Hori T, Takahashi T (2000) Presynaptic inhibition by Muscimol through $GABA_B$ receptors. Eur J Neurosci 12:3433-3436.